

J. YOO^{1,✉}
T. LEE²
J.B. JEFFRIES¹
R.K. HANSON¹

Detection of trace nitric oxide concentrations using 1-D laser-induced fluorescence imaging

¹ High Temperature Gasdynamics Laboratory, Department of Mechanical Engineering, Stanford University, Stanford, CA 94305, USA

² Department of Mechanical Engineering, Michigan State University, East Lansing, MI 48824-1226, USA

Received: 29 November 2007/

Revised version: 28 February 2008

Published online: 6 May 2008 • © Springer-Verlag 2008

ABSTRACT Spectrally resolved laser-induced fluorescence (LIF) with one-dimensional spatial imaging was investigated as a technique for detection of trace concentrations of nitric oxide (NO) in high-pressure flames. Experiments were performed in the burnt gases of premixed methane/argon/oxygen flames with seeded NO (15 to 50 ppm), pressures of 10 to 60 bar, and an equivalence ratio of 0.9. LIF signals were dispersed with a spectrometer and recorded on a 2-D intensified CCD array yielding both spectral resolution and 1-D spatial resolution. This method allows isolation of NO-LIF from interference signals due to alternative species (mainly hot O₂ and CO₂) while providing spatial resolution along the line of the excitation laser. A fast data analysis strategy was developed to enable pulse-by-pulse NO concentration measurements from these images. Statistical analyses as a function of laser energy of these single-shot data were used to determine the detection limits for NO concentration as well as the measurement precision. Extrapolating these results to pulse energies of ~ 16 mJ/pulse yielded a predicted detection limit of ~ 10 ppm for pressures up to 60 bar. Quantitative 1-D LIF measurements were performed in CH₄/air flames to validate capability for detection of nascent NO in flames at 10–60 bar.

PACS 42.62.Fi; 42.30.Va; 47.70.Pq; 07.35.+k; 39.30.+w

1 Introduction

Emission of nitric oxide (NO) is a major concern for air-breathing combustion systems as NO is an important pollutant formed in the oxidation of fossil fuels [1, 2]. Along with sulfur oxides, carbon compounds and particulate matter, NO_x gases are identified as a cause of severe health and environment hazards [1, 3, 4]. Thus, minimizing the production of these harmful byproducts is a key design parameter for modern-day combustion systems. The formation of NO in flames has been extensively studied and well-documented in the literature, e.g., [2, 5]. This progress coupled with the need to satisfy legislative restrictions has led to burners that produce low NO emissions (< 50 ppm) [6]. As most practi-

cal combustion systems for propulsion and power generation applications (i.e., IC engines, gas turbines, etc.) operate under high-pressure conditions, trace detection of NO at elevated pressures is an important diagnostic target to facilitate continuing combustion research.

Here we investigate 1-D, spectrally resolved, non-intrusive optical detection of trace NO using laser-induced-fluorescence (LIF) at elevated pressure conditions. The unique properties of laser light enable selective and quantitative probing of chemical species [7, 8], and LIF detection of nitric oxide is a well-established tool for detection of NO in both practical combustion systems and laboratory flames. For diagnostics of practical combustion systems, NO-LIF measurements to date have mostly been made using the *A–X* electronic system with transitions in the (0,0), (0,1) or the (0,2) bands at 226, 235 and 248 nm, respectively [9–11]. Measurements have also been made using *D–X* (0,1) transitions at 193 nm [12], and more recently, two-photon NO-LIF of *A–X* (0,0) was applied to an optical diesel engine [13]. However, the strategy investigated in the current study was based on *A–X* (0,0) excitation of NO, as it has the highest LIF signal output and reduces absorption by CO₂ compared to the *D–X* system.

This work builds on past research on LIF of NO in high-pressure combustion gases using *A–X* excitation [14–21]. A detailed analysis and comparison of *A–X* excitation strategies in high-pressure flames (1–60 bar) was published previously [18], and the complications of pressure broadening, strong attenuation of UV light by CO₂ absorption [22], and the interference LIF of O₂ and CO₂ have been discussed in detail [14–21].

Here we extend past work to lower concentrations of NO and determine the single-shot detection limits for spectrally resolved LIF in the burned gases of fuel-lean high-pressure flames. NO is seeded in premixed CH₄/O₂ flames diluted in argon to match the heat capacity of CH₄/air without the production of nascent NO. Our NO-LIF line-imaging technique was used previously with large (300 ppm) NO concentrations and pulse averaging, with the goal of optimizing fluorescence filters for 2D-LIF imaging of NO [23]. By contrast, the current study focused on the determination of single-shot detection limits for trace NO concentration levels by the 1-D line-imaging method and the development of a rapid data analysis scheme. Single-shot and laser-pulse averaged 1-D NO-LIF

✉ Fax: +1-650-7231748, E-mail: jhyoo@stanford.edu

measurements were then made in a premixed CH_4/air flame to test the method on nascent NO concentrations. To validate the 1-D LIF NO concentration measurement capability, these data were compared with detailed kinetic calculations and measurements using an NO addition method.

2 Experimental setup

The experimental setup shown in Fig. 1 used a high-pressure flame apparatus described previously [18–21]. Laminar, premixed flat flames at pressures from 10 to 60 bar were stabilized on a porous, sintered stainless-steel plate of 8 mm diameter. The burner was mounted in a stainless-steel housing with an inner diameter of 60 mm; the pressure was stabilized to ± 0.1 bar [18, 20, 21]. The fuel was methane and the oxidizer was a mixture of 20% oxygen and 80% argon, chosen to approximate the heat capacity of normal air while suppressing nascent NO generation (by replacing nitrogen with argon). All measurements were carried out with fuel/oxidizer equivalence ratios of $\varphi = 0.9$. Tests were performed for 15, 25, 35, and 50 parts per million NO seeded into the feedstock gases.

Optical access to the flame was possible through four quartz windows (Heraeus, Suprasil 2 Grade) placed at right angles on the burner. Laser pulse energy ranged from 0.7–1.1 mJ/pulse (7 ns pulses at 10 Hz with a linewidth of 0.4 cm^{-1}) from a Nd:YAG-pumped (Quanta Ray GCR250), frequency-doubled (BBO), dye laser (LAS, LDL205). The laser was tuned near 226.03 nm to the blend of rotational transitions ($P1(23.5)$, $Q1 + P21(14.5)$, $Q2 + R12(20.5)$) in the NO $A-X$ ($v' = 0, v'' = 0$) band identified in our previous work to minimize the interference from O_2 LIF [15, 18].

The optical detection was modified from our earlier work to provide spectrally resolved 1-D line imaging measurements, and the laser beam was collimated (diameter = 1 mm) along a line 3 mm above the burner matrix, crossing the flame horizontally as seen in Fig. 1. Even though the seeded NO was mostly converted to NO_2 in the flame front, model calculations show that the NO concentration recovered to the seeded concentration value within 1.5 mm above the burner matrix. Thus the NO concentration at the measurement lo-

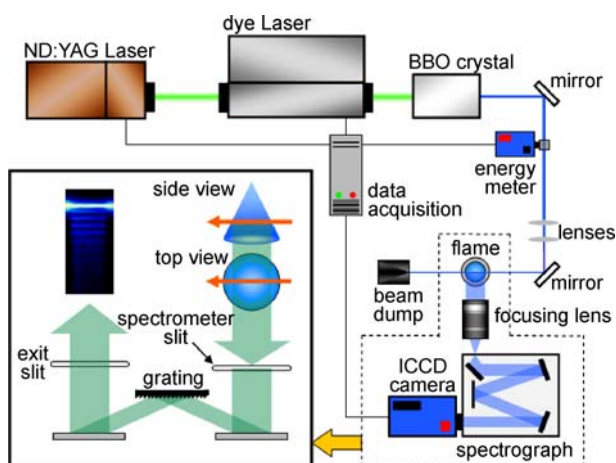


FIGURE 1 Setup for 1-D spectrally resolved LIF measurements in the high-pressure burner

cation (3 mm above the matrix) was equal to the seeded NO concentration in the fuel-lean $\text{CH}_4/\text{Ar}/\text{O}_2$ flames. Fluorescence signals were collected at right angles to the laser beam and focused with an $f/4.5$, $f = 105$ mm achromatic UV lens (Nikon) onto the horizontal entrance slit ($200 \mu\text{m}$) of an imaging spectrometer (McPherson, Chromex 250IS) equipped with a 300 grooves/mm grating blazed at 250 nm, used in first order. Faster UV collection lenses are commercially available (e.g., Halle $f/2$ [24]) that could increase photon collection more than a factor of 4 and thereby improve shot-noise-limited detection limits.

The spectrally resolved fluorescence signals exiting the spectrometer were imaged onto an intensified CCD camera (LaVision DynaMight), with fluorescence wavelength on the abscissa and position along the laser beam on the ordinate. The signal was collected single-shot or summed-on-chip to simulate experiments with larger excitation pulse energy. The latter technique simulated conditions with higher laser pulse energy than available from our current Nd:YAG and dye laser system without adding extra read-noise from the camera. The temperature of the ICCD was controlled by external cooling, and the pulse energy was measured with a fast photodiode (La Vision).

3 1-D line imaging data evaluation

3.1 Evaluation of 1-D line-images

Real-time evaluation of LIF spectra in post-combustion gases is possible with single-shot imaging. Thus, a robust and rapid detection strategy was developed to extract

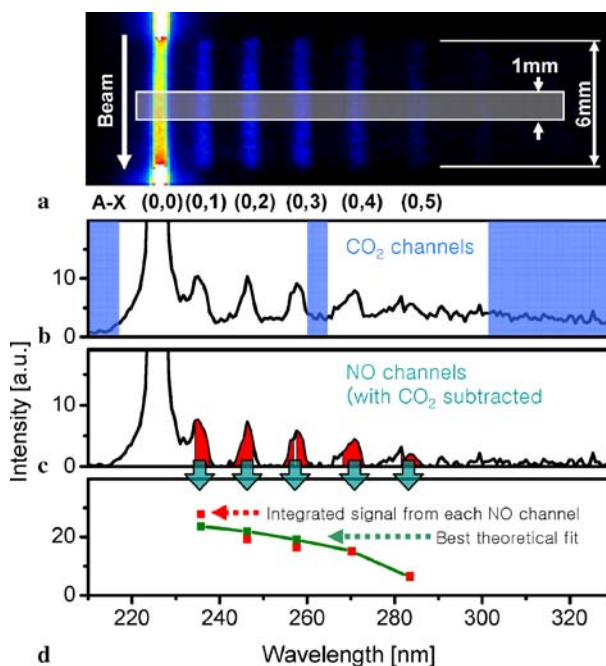


FIGURE 2 (a) Background-corrected single-shot LIF image from the ICCD for a 60 bar $\text{CH}_4/\text{Ar}/\text{O}_2$ flame with 50 ppm of seeded NO. The LIF spectrum averaged from 100 single-shot images and integrated over the center 1 mm is shown in (b) along with the three CO_2 data channels (see text). (c) The residual signal in the NO data channels following subtraction of the contribution from CO_2 LIF. (d) The best theoretical fit for the relative LIF signal strength of each channel for the measured data

1st channel	210–216 nm
2nd channel	261–265 nm
3rd channel	305–330 nm

TABLE 1 CO₂ channel spectral location

Band	NO band [nm]	NO channel [nm]	Percentage of NO fluorescence [%]
0–1	233.1–237.2	234.4–237.2	99
0–2	242.9–248.1	242.9–247.5	85
0–3	254.0–259.9	254.0–256.9	92
		257.5–259.9	
0–4	267.7–272.6	268.4–272.6	99
0–5	280.7–286.3	281.3–286.3	99

TABLE 2 NO channel spectral location and percentage of NO fluorescence captured for 1800 K and 40 bar pressure

NO-LIF intensities from the LIF image. An image of the background noise from the camera’s ICCD array, taken without laser excitation, was automatically subtracted from an LIF image. An example of the resulting single-shot LIF image from a 60 bar flame with 50 ppm of added NO is shown in panel A of Fig. 2; note that the 1-D spatial information along the laser beam is on the ordinate. Data from the center 1 mm of the flame were spatially integrated to obtain the wavelength-resolved fluorescence spectra in the lower three panels. The vibrational bands of the NO fluorescence were obvious in the data; however, the fluorescence in the (0,0) band was obscured by Rayleigh scattering.

We assume that the measured fluorescence spectrum contained superimposed LIF signals from NO, O₂, and CO₂ [23]. To account for the effects of CO₂-LIF, which is a broadband emission across the entire region [25], the CO₂ contribution was determined by the signal in these CO₂ channels (the wavelength regions are listed in Table 1). Spectral simulations [26] predict the signal in these channels to be dominated by CO₂ LIF, and the NO and O₂ LIF in these regions to be minimal. The broadband CO₂ contribution to the LIF signal is linearly interpolated between the CO₂ channels, and subtracted from the data. The five NO channels listed in Table 2 correspond to portions of the (0,1), (0,2), (0,3), (0,4) and (0,5) NO vibrational bands. The spectral width of each channel was optimized using the simulation of the NO and O₂ fluorescence given by LIFsim [26], to minimize the interference from O₂, and the fluorescence signal in each channel was integrated.

The ratio of the integrated signals from each NO channel was governed by the Franck–Condon factors for each band, weighted by the overlap of each NO band with selected NO channel regions and corrected for the spectral response of the data collection system (collection lens, spectrometer, and ICCD camera) measured with a calibrated D₂ lamp [18].

The bottom plot in Fig. 2, compares the measured average of 100 shots in the NO channels with the best theoretical fit. One test of the NO concentration measured from this fitting scheme is illustrated in Fig. 3. Experiments at 60 bar were conducted for NO seeding between 15 and 50 ppm and for a range of accumulated number of images summed on the detector. The linear response of the NO-LIF signal intensity with the number of imaged averaged for different amounts of seeded NO (i.e., the slopes of the lines in Fig. 3 are the same

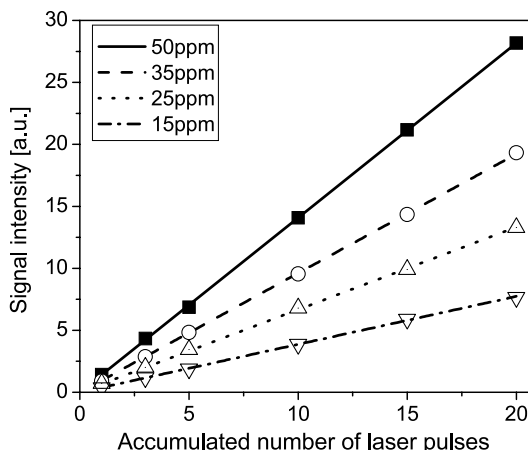


FIGURE 3 NO-LIF signal for CH₄/Ar/O₂ flame, $\phi = 0.9$, for 15, 25, 35, and 50 ppm seeded NO at 60 bar pressure as a function of number of laser pulses summed on-chip. The nominal pulse energy is 0.8 mJ/pulse

per ppm of NO) provides confidence that our data reduction scheme was not contaminated with O₂ or CO₂ interference.

3.2 Noise evaluation

Noise evaluation was crucial to defining the detection limits of 1-D LIF achieved with the data reduction algorithm, and accurate assessment of noise became more important as the NO-LIF signal levels became small. Single-shot data were collected for each pressure and NO seeding level. Measurement noise was calculated from the absolute difference between the spectrally integrated single-shot (background and CO₂-corrected) NO spectrum over the 5 NO channels and the 100-shot average data. Three significant contributions to the noise were observed: thermal, read, and shot noise. Thermal noise is due to thermal background on the ICCD array. Read noise is system-specific and scales with the readout rate. This camera-specific background noise was suppressed by subtracting a background image taken without laser excitation just prior to each laser-excited image. Shot noise is due to the finite number of signal photons reaching the CCD array, causing statistical fluctuation in the measurement. This form of noise follows Poisson statistics and scales with the square root of incoming photons (or laser energy). Shot noise was confirmed to be the major contributor to measurement uncertainty for the experiments performed here.

The LIF intensity noise at different pressures and accumulated number of laser pulses for seeded NO concentrations of 50 ppm is plotted in Fig. 4. The accumulation of multiple shots on the CCD chip is used to simulate higher laser pulse energies. All data points scaled with the half power of the total laser energy, confirming that the experimental setup was shot-noise limited.

Figure 5 shows the percentage standard deviation of the concentration measurement for an ensemble of 100 single-shot images at 0.8 mJ/pulse laser energy, for each pressure and seeding level. The percentage standard deviation is seen to increase with increasing pressure and decreasing seeded NO concentration, as expected.

To simulate higher laser pulse energies, multiple shots were summed on the CCD. This approach assumed that the

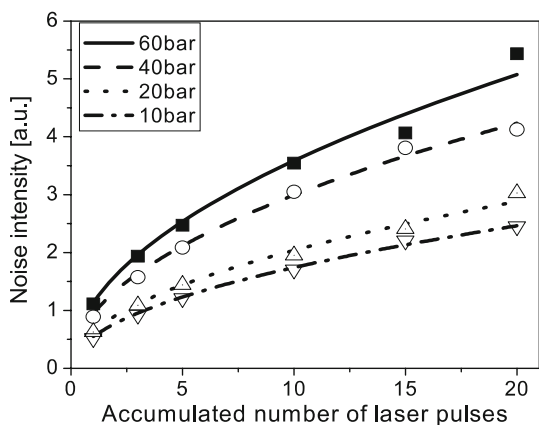


FIGURE 4 LIF intensity noise (see text) defined as the average deviation from the measured average of 100 on-chip accumulations. Single-pulse energy of 0.8 mJ for $\text{CH}_4/\text{Ar}/\text{O}_2$ flame, $\varphi = 0.9$, 50 ppm NO seeded flame, and 10, 20, 40, and 60 bar

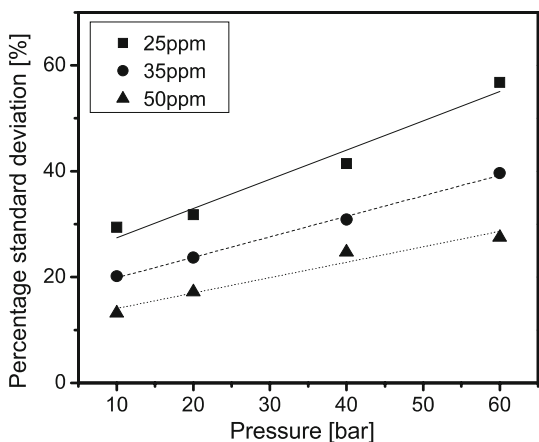


FIGURE 5 Percentage standard deviation of single-shot NO concentration measurement in $\text{CH}_4/\text{Ar}/\text{O}_2$, $\varphi = 0.9$ flame at 10, 20, 40, and 60 bar pressure, and 25, 35, and 50 ppm seeded NO

higher laser energy excitation was in the linear regime for LIF. Thus, care was taken to limit the number of accumulated shots so as to not exceed the equivalent laser energy required to saturate the NO-LIF signal. The saturation limit of the laser energy was estimated using a simple two-level steady-state model. For our conditions, the beam diameter was 1 mm and the wavelength was 226.03 nm ($P_1(23.5)$, $Q_1 + P_{21}(14.5)$, $Q_2 + R_{12}(20.5)$); the spectroscopic database of NO from LIFsim [26] was utilized in our simulations. This model yields a value of 12 mJ/pulse for the laser energy needed to saturate the NO-LIF signal at 10 bar and 73 mJ/pulse to saturate at 60 bar. The actual limits are expected to be considerably larger when one applies a more realistic model accounting for the effects of rotational transfer [26].

4 Results and discussion

NO-LIF data were collected for flames between 10 and 60 bar and NO concentrations between 15 and 50 ppm with $\varphi = 0.9$, and statistical studies of these data were used to determine detection limits for the 1-D line-imaging technique. 100 LIF images of 1, 3, 5, 10, 15, and 20 laser pulses accumulated on the camera were taken for 15 specific condi-

tions, and a total of 9000 images were analyzed. For any given condition, 100 images were averaged to provide the theoretical relative intensity (as illustrated in Fig. 2). The observed NO signals were linear in laser pulse energy and seeded NO concentration enabling direct comparison between any two test conditions. Statistical studies were then conducted to define minimum detection limits. Although we did not perform a complete study of the variation of these detection limits with fuel/air equivalence ratio, we can predict how the detection limit will vary. For fuel-rich flames, there is no oxygen in the burned gases and without the oxygen LIF interference disappears. There are many more choices of excitation wavelength providing increased signal and thus reducing the shot-noise limited NO detection limit. As the equivalence ratio becomes larger ($\varphi > 1.5$), we reported in [25] the formation of polyatomic molecules (possibly PAH), which provide severe interference. For $\varphi < 0.9$ the oxygen interference increases, thus making for a larger NO detection limit, but our choice of excitation wavelengths remains optimized.

4.1 Signal to noise ratio

SNR was determined for all test conditions, defined as a ratio of NO-LIF signal to average noise intensity as illustrated in Fig. 2. For the shot-noise-limited case, the SNR is expected to scale with the square root of laser pulse energy. Figure 6 illustrates that the measured SNR agrees with this expectation.

4.2 Measurement uncertainty

The measurement uncertainty was defined as the standard deviation of NO concentration determined from an ensemble of 100 measurements at a given pressure and laser energy. Figure 7 illustrates the expected increase in the fractional standard deviation with decreasing NO-LIF signal strength. For large NO concentrations, of course, the fractional standard deviation increases less with smaller laser energy. Effective single-shot measurements of small NO concentration values will obviously require large laser pulse energies, as expected for shot-noise-limited SNR.

4.3 Minimum detection limit

The observed SNR and measurement uncertainty can be combined to yield an estimate of the minimum detection limit characteristics. Figure 8 provides guidelines for selecting appropriate laser energy for the lowest detectable NO concentration and its measurement uncertainty. By virtue of being shot-noise limited, the measurement can be projected to higher laser energy by on-chip summation of multiple pulses, provided that the equivalent laser pulse energy remains within the NO-LIF linear regime and assuming there are negligible non-linear effects, as expected.

As illustrated in Fig. 8, the detection limit and measurement error decreased as more laser pulses were integrated on-chip (corresponding to higher equivalent laser pulse energy) and lower pressure. The minimum detectable NO concentration inferred from our analysis was ~ 5 ppm at 10 bar pressure, for 4 mJ/pulse laser energy, and using our $f/4.5$

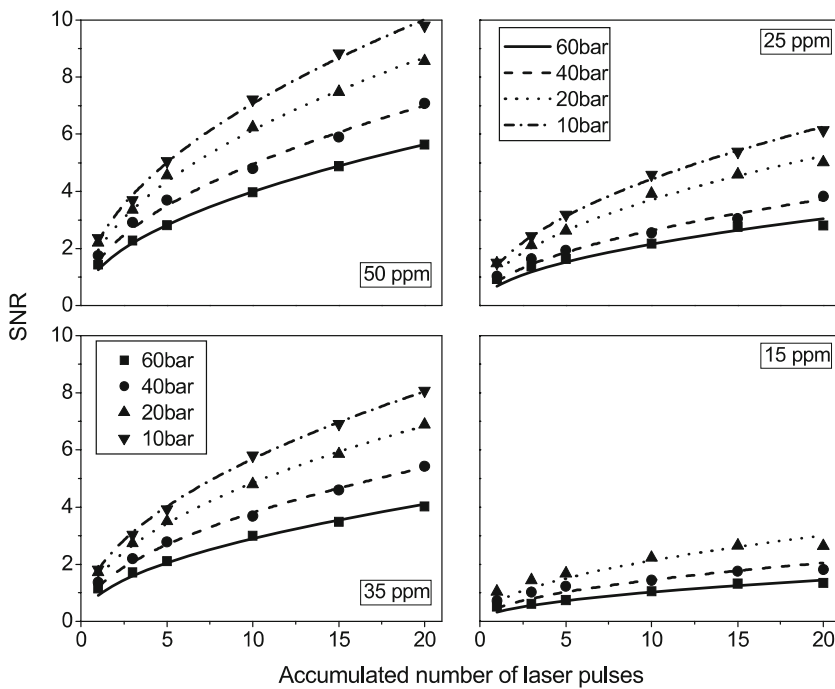


FIGURE 6 SNR of NO concentration measurement in CH₄/Ar/O₂, $\phi = 0.9$ flame for 15, 25, 35, and 50 ppm seeded NO concentration at 10, 20, 40, and 60 bar pressure

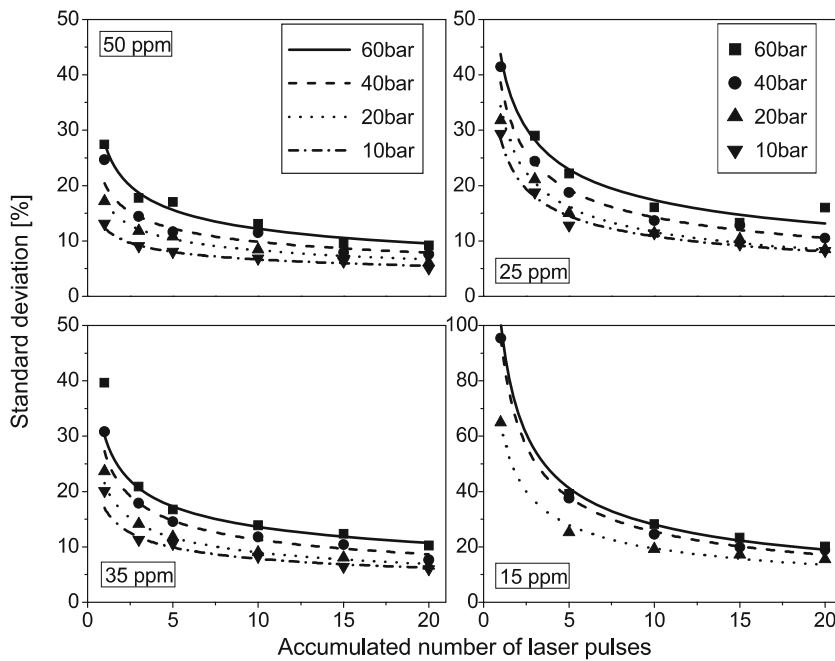


FIGURE 7 Shot-to-shot analysis for CH₄/Ar/O₂, $\phi = 0.9$ flame for 15, 25, 35, and 50 ppm seeded NO concentration at 10, 20, 40, and 60 bar pressure

collection lens. Higher laser energies at 10 bar yield lower detection limits, though caution is needed to ensure that the NO-LIF signal is still sufficiently in the linear excitation regime. For 60 bar, the minimum detectable NO concentration was ~ 10 ppm at 16 mJ laser pulse energy, a value well below saturation. This narrow-band laser energy at 226 nm is feasible with current commercial Nd:YAG-pumped dye or OPO lasers.

4.4 Nascent NO in premixed CH₄/air flames

Measurements of nascent NO in a premixed CH₄/air flame were used to test our NO detection strategy. Here

the current 1-D NO-LIF concentration detection method was compared with the 2-line NO addition method used previously [27], applied to a CH₄/air flame at 1, 10, 20, 40, and 60 bar without NO seeding. This use of two different excitation wavelengths was shown earlier [27] to provide quantitative NO concentrations in high-pressure flames. However, the 2-line NO addition method requires significant averaging and cannot be used for single-shot applications. Nascent NO concentrations based on the 1-D NO-LIF method are calibrated by comparing NO signals in the CH₄/air flame against those of the CH₄/Ar/O₂ flame with 100 ppm seeded NO at each pressure condition. Figure 9 shows that the 1-D NO-LIF measurements are in excellent agreement with the 2-line NO

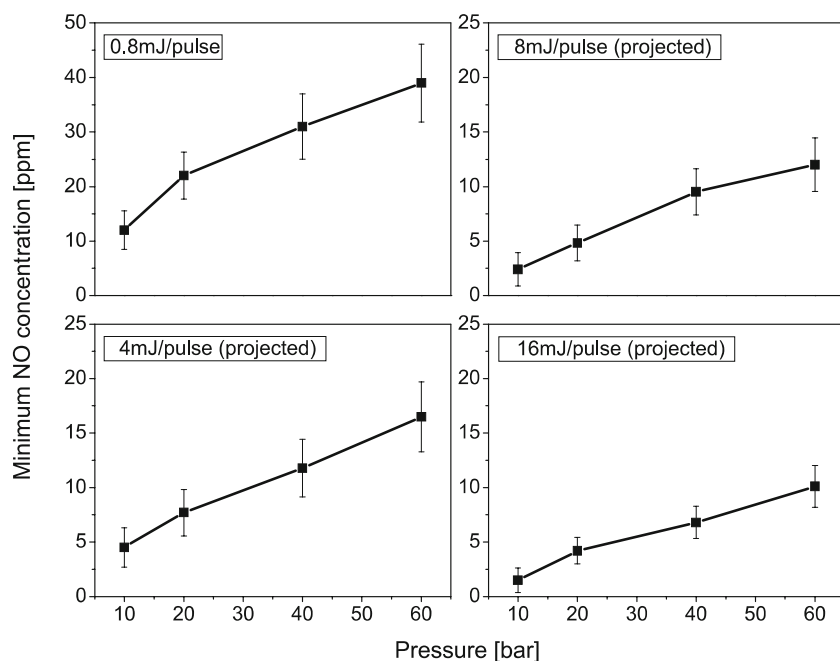


FIGURE 8 Minimum detectable NO concentration for 0.8 mJ/pulse (single-shot), 4 mJ/pulse (projected, by summing 5 shots), 8 mJ/pulse (projected by summing 10 shots), and 16 mJ/pulse (projected by summing 20 shots) for $\text{CH}_4/\text{Ar}/\text{O}_2$, $\varphi = 0.9$, flame at 10, 20, 40, and 60 bar

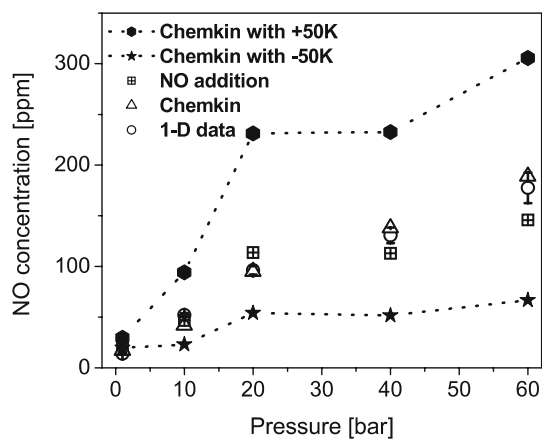


FIGURE 9 Comparison of measured single-shot nascent NO concentrations in CH_4/air flames, 3 mm above the burner matrix, by the 1-D NO-LIF and the NO addition technique. Simulations are shown using the Chemkin Premix 1-D flame code (GRI-Mech 3.0) with no NO seeding ($\varphi = 0.9$), based on the measured temperature and also with temperature varied by ± 50 K

addition method from [27]. Measurements from the 1-D NO-LIF method and the 2-line NO addition method are all in excellent agreement with predictions from Premix calculations using Chemkin [23] and the GRI-Mech 3.0 chemical mechanism. The Premix calculation was constrained by the measured temperature profile taken from [27]. The model calculations are extremely sensitive to gas temperature, as indicated by varying the temperature by ± 50 K. Hence, although the measurements are in good agreement with the kinetics modeling, this is not a sensitive validation tool. However, most importantly, the excellent agreement between the two measurement techniques provides confidence in the new 1-D LIF method.

4.5 Spatial resolution

1-D NO-LIF offers the potential for spatially and temporally resolved measurements of the NO concentration

along the path of the laser beam. The laser beam was aligned parallel to the burner matrix and parallel to the slit of the spectrometer, and the NO-LIF signal intensity along the path of the laser beam was resolved by scanning the data collection window across the ICCD image (upper panel of Fig. 2). These spatially resolved single-shot measurements were corrected for attenuation by CO_2 , and an example for a 20 bar flame is shown in Fig. 10. The images were taken with an $f/4.5$ collection lens and imaged onto a 1024×1024 ICCD array with $13 \times 13 \mu\text{m}$ pixel size to increase the modulation transfer function (MTF), which in turn increases the resolving power. The CCD data was binned by summing four adjacent pixels along spatial axis and two pixels along the spectral axis without loss in resolution due to its point spread function (PSF). If we project the size of the four-binned pixels through the collection optics magnification onto the laser beam axis we find a 0.13 mm spatial resolution (ten times larger than an individual pixel). The spectrometer slit width of $200 \mu\text{m}$ is overfilled by the image of the 1 mm diameter laser beam.

5 Conclusions

The detection limits for NO concentration measured by 1-D line imaging of $A-X$ NO-LIF were determined as a function of pressure in the burned gases of premixed specific mixture flames with small NO concentrations. Statistical analysis of images confirmed that shot noise is the dominant source of uncertainty. The detection limit and corresponding measurement error were investigated. Guidelines were developed to select the appropriate laser energy for lowest detectable NO concentration and measurement accuracy. The results indicate that for practical application where NO concentrations may be on the order of 10 ppm, laser pulse energies of 16 mJ/pulse can provide < 10 ppm detection limits for flames up to 60 bar. Tests of the strategy to measure the nascent NO in premixed CH_4/air flames were in good

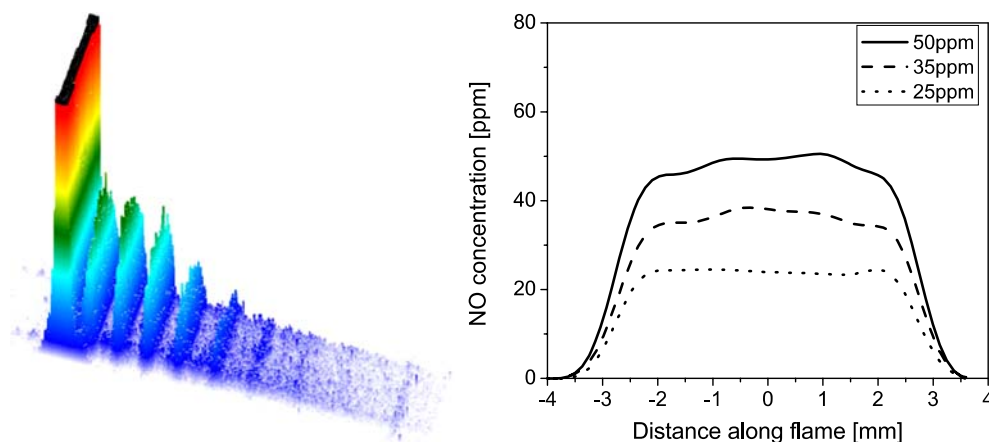


FIGURE 10 Spatially resolved single-shot NO concentration measurement across $\text{CH}_4/\text{Ar}/\text{O}_2$, $\phi = 0.9$ flame for 25, 35, and 50 ppm seeded NO concentration at 20 bar pressure

agreement with Chemkin calculations and two-line excitation measurements.

ACKNOWLEDGEMENTS We gratefully acknowledge support from the Air Force Office of Scientific Research (AFOSR) with Dr. Julian Tishkoff as technical monitor.

REFERENCES

- J. Warnatz, U. Maas, R.W. Dibble, *Combustion*, 3rd edn. (Springer, Berlin Heidelberg New York, 1997)
- C.T. Bowman, *Proc. Combust. Inst.* **24**, 859 (1992)
- J.H. Seinfeld, S.N. Pandis, *Atmospheric Chemistry and Physics: From Air Pollution to Climate Change* (Wiley-Interscience, New York, 1997)
- J.A. Miller, C.T. Bowman, *Prog. Energ. Combust. Sci.* **15**, 287 (1989)
- C.T. Bowman, Gas-phase reaction mechanisms for nitrogen oxide formation and removal in combustion, in *Pollutants from Combustion*, ed. by C. Vovelle (Kluwer, Dordrecht, 2000), pp. 123–144
- M.S. Smith, L.L. Price, W.D. Williams, *AIAA J.* **31**, 478 (1993)
- A.C. Eckbreth, *Laser Diagnostics for Combustion Temperature and Species* (Gordon and Breach, Amsterdam, 1996)
- K. Kohse-Höinghaus, J.B. Jeffries, *Applied Combustion Diagnostics* (Taylor and Francis, London, 2002)
- J.E. Dec, R.E. Canaan, SAE Tech. Paper Series 900147 (1998)
- P. Jamette, P. Desgroux, V. Ricordeau, B. Deschamps, SAE Tech. Paper Series 2001-01-1926 (2001)
- C. Schulz, V. Sick, U.E. Meier, J. Heinze, W. Stricker, *Appl. Opt.* **38**, 1434 (1999)
- P. Andresen, G. Meijer, H. Schluter, H. Voges, A. Koch, W. Hentschel, W. Oppermann, W. Rothe, *Appl. Opt.* **29**, 2392 (1990)
- G.C. Glen, C.J. Mueller, C.F. Lee, *Appl. Opt.* **45**, 2089 (2006)
- A.O. Vyrodov, J. Heinze, M. Dillman, U.E. Meier, W. Stricker, *Appl. Phys. B* **61**, 409 (1995)
- M.D. DiRosa, K.G. Klavuhn, R.K. Hanson, *Combust. Sci. Technol.* **118**, 257 (1996)
- W.P. Patridge, M.S. Klassen, D.D. Thomsen, N.M. Laurendeau, *Appl. Opt.* **34**, 4890 (1996)
- D.D. Thomsen, F.F. Kuligowski, N.M. Laurendeau, *Appl. Opt.* **36**, 3244 (1997)
- W.G. Bessler, C. Schulz, T. Lee, J.B. Jeffries, R.K. Hanson, *Appl. Opt.* **42**, 4922 (2003)
- W.G. Bessler, Quantitative nitric oxide concentration and temperature imaging in flames over a wide pressure range with laser-induced fluorescence, Dissertation, Physikalisch-Chemisches Institut, University of Heidelberg (2003)
- W.G. Bessler, C. Schulz, T. Lee, J.B. Jeffries, R.K. Hanson, *Appl. Opt.* **41**, 3547 (2002)
- W.G. Bessler, C. Schulz, T. Lee, J.B. Jeffries, R.K. Hanson, *Appl. Opt.* **42**, 2031 (2003)
- C. Schulz, J.B. Jeffries, D.F. Davidson, J.D. Koch, J. Wolfrum, R.K. Hanson, *Proc. Combust. Inst.* **29**, 2725 (2002)
- T. Lee, J.B. Jeffries, R.K. Hanson, *Proc. Combust. Inst.* **31**, 757 (2006)
- H. Kronemayer, K. Omerbegovic, C. Schulz, *Appl. Opt.* **46**, 8322 (2007)
- W.G. Bessler, C. Schulz, T. Lee, J.B. Jeffries, R.K. Hanson, *Chem. Phys. Lett.* **375**, 344 (2003)
- W.G. Bessler, C. Schulz, V. Sick, J.W. Daily, A versatile modeling tool for nitric oxide LIF spectra, in 3rd Joint Meeting US Sec. Combust. Inst., Chicago (2003), <http://www.lifsim.com>, accessed 2007
- T. Lee, W.G. Bessler, H. Kronemayer, C. Schulz, J.B. Jeffries, *Appl. Opt.* **44**, 6718 (2005)